RESEARCH ARTICLE

Investigation of Olive Leaf Polyphenol Extract Loaded Silver Nanoparticle Optimization by Box-Behnken Design

Renganathan A*, Srinivasan R

Department of Pharmaceutical Chemistry, Faculty of Pharmacy, Bharath Institute of Higher Education and Research, Chennai, Tamil Nadu, India

Received: 12th March, 2024; Revised: 03rd May, 2024; Accepted: 22nd August, 2024; Available Online: 25th September, 2024

ABSTRACT

Silver nanoparticles (AgNPs) are synthesized and optimized by reducing and stabilizing them with olive leaf extract. The successful synthesis of AgNPs was verified by UV-vis spectroscopy, SEM imaging, and DLS measurements, demonstrating characteristic features such as a surface plasmon resonance peak, spherical morphology, crystalline structure, and narrow size distribution with good stability. Utilizing Box-Behnken Design (BBD), the optimal synthesis conditions were determined, with a silver nitrate concentration of 1 mM, olive leaf extract volume of 10 mL, and reaction time of 60 minutes, yielding AgNPs with desirable properties. Statistical analysis revealed the significant influence of individual variables and their interactions on AgNP characteristics. Lower concentrations of silver nitrate and olive leaf extract led to smaller particle sizes and higher zeta potentials, while longer reaction times resulted in larger particles and lower zeta potentials. Among the experimental runs, Run 11 exhibited the most favorable properties, with 54 nm particle size, -36 mV zeta potential, and an encapsulation efficiency of 92.28%. ANOVA analysis further elucidated the significant effects of synthesis parameters on zeta potential, particle size, and encapsulation efficiency. In conclusion, the optimized formulation obtained through BBD offers a tailored approach for the synthesis of AgNPs with desired properties, suitable for various applications such as biomedical, catalytic, and sensing applications. The comprehensive understanding of synthesis parameters and their effects provided by this study facilitates the rational design of AgNPs for specific applications, enhancing their potential in diverse fields.

Keywords: Olive leaf extract, Polyphenols, Silver nanoparticles, Box-Behnken design, Optimization, Nanotechnology.

International Journal of Drug Delivery Technology (2024); DOI: 10.25258/ijddt.14.3.09

How to cite this article: Renganathan A, Srinivasan R. Investigation of Olive Leaf Polyphenol Extract Loaded Silver Nanoparticle Optimization by Box-Behnken Design. International Journal of Drug Delivery Technology. 2024;14(3):1312-1322.

Source of support: Nil.

Conflict of interest: None

INTRODUCTION

Olive leaf extracts contain polyphenols, particularly oleuropein, which has significant antipsoriatic,[1] antimicrobial, antioxidant, and anti-inflammatory effects.[2,3] The incorporation of these extracts into silver nanoparticles enhances their stability and bioavailability, offering a novel approach to therapeutic applications. Silver nanoparticles themselves have well-documented antimicrobial properties, making the combination a potent tool for various biomedical applications.[4]

Olive leaf extracts are made from olive leaves (*Olea europaea*), which are used in traditional medicine for their therapeutic properties. The extracts are particularly high in polyphenolic compounds, which are powerful antioxidants, antimicrobials, and anti-inflammatory agents. These bioactive compounds have been extensively studied for their health benefits and potential applications in various diseases, including chronic inflammatory conditions like psoriasis.[5] Olive leaf extracts contain the following polyphenolic compounds:

Oleuropein

This compound has been studied extensively in olive leaves. Oleuropein has demonstrated significant antioxidant and anti-inflammatory properties that can reduce inflammation and oxidative stress.[6]

Hydroxytyrosol

A potent antioxidant, hydroxytyrosol inhibits free radical formation and protects cells against oxidative damage. Additionally, it has anti-inflammatory properties that can improve skin health.

Tyrosol

Similar to hydroxytyrosol, tyrosol exhibits strong antioxidant properties and contributes to the overall health benefits of olive leaf extracts.

Flavonoids

Compounds found in olive leaves include luteolin and apigenin, which have anti-inflammatory and antioxidant activities.

*Author for Correspondence: meetrenganathan@gmail.com

Verbascoside

Another important polyphenol with demonstrated antioxidant, anti-inflammatory, and antimicrobial properties.[7,8]

Psoriasis can be defined as a chronic autoimmune disease that results in hyperproliferation of keratinocytes and chronic inflammation. The underlying mechanisms involve oxidative stress, an overactive immune response, and abnormal keratinocyte behavior.[9]

Polyphenolic compounds from olive leaf extracts can modulate these pathways through several mechanisms.[10,11]

Antioxidant Activity

Polyphenols, particularly oleuropein and hydroxytyrosol, are powerful antioxidants that can scavenge free radicals, reducing oxidative stress. This is crucial in psoriasis, where oxidative stress is a key factor in the disease's pathogenesis. By neutralizing reactive oxygen species (ROS), these compounds help protect skin cells from damage and reduce inflammation.

Anti-inflammatory Effects

Polyphenols such as oleuropein reduce the production of pro-inflammatory cytokines like TNF-α, IL-6, and IL-1β. This helps to modulate the immune response and reduce the inflammatory processes that contribute to the development and exacerbation of psoriatic lesions.

Modulation of Immune Response

Olive leaf polyphenols influence the activity of immune cells such as T cells and dendritic cells. By modulating these cells' functions, the extracts help balance the immune response, which is often dysregulated in psoriasis.

Inhibition of Keratinocyte Proliferation

Some studies suggest that olive leaf polyphenols can inhibit the abnormal proliferation of keratinocytes, which is a hallmark of psoriasis. This helps in reducing the thickening and scaling of the skin associated with psoriatic plaques.

Antimicrobial Properties

The antimicrobial activity of olive leaf polyphenols, particularly oleuropein, can help manage secondary infections in psoriatic lesions. This is important as infections can exacerbate psoriasis symptoms.

The integration of olive leaf polyphenols into psoriasis treatment shows promise due to their natural, multifaceted properties. These compounds offer a safe alternative to synthetic drugs, with potential benefits in addressing various aspects of the disease. Advanced delivery systems, like nanoparticles, further enhance their therapeutic efficacy. However, further research, including clinical trials and formulation development, is needed to fully realize their potential in psoriasis therapy. The bioactive polyphenolic compounds from olive leaf extracts offer significant potential for the treatment of psoriasis. Their antioxidant, anti-inflammatory, and immunomodulatory properties address key pathogenic mechanisms in the disease, making them promising candidates for developing novel, effective, and safe therapeutic strategies. Psoriasis is an autoimmune condition characterized by thick, red, scaly patches of skin. Traditional treatments, including topical agents, systemic medications, and biologics, have varying degrees of efficacy and side effects. Recently, nanotechnology has generated significant interest, particularly silver nanoparticles (AgNPs), for dermatological applications due to their unique properties, such as antimicrobial properties and anti-inflammatory properties. The integration of herbal medicine into nanotechnology offers a promising avenue for psoriasis treatment. Herbal drugs, known for their therapeutic benefits and minimal side effects, can be optimized when delivered via nanoparticles. This study aims to develop and evaluate an herbal drug-loaded silver nanoparticle-enriched gel for its antipsoriatic effect in an animal model.[10-12]

The optimization of nanoparticle synthesis is crucial for achieving desired particle sizes, stability, and drug-loading efficiency. The Box-Behnken design (BBD) is an effective statistical technique for optimizing complex processes with multiple variables. This study utilizes BBD to optimize the synthesis conditions of olive leaf polyphenol extract-loaded AgNPs.[13]

This study is based on the hypothesis that the incorporation of olive leaf polyphenol extracts into silver nanoparticles will enhance the stability, bioavailability, and therapeutic efficacy of the nanoparticles, particularly in terms of antioxidant, antimicrobial, and anti-inflammatory properties. The hypothesis further posits that optimizing the synthesis conditions of these nanoparticles using the Box-Behnken design (BBD) will yield nanoparticles with the desired properties, such as optimal particle size, stability, and high encapsulation efficiency, making them suitable for various biomedical applications.

The primary objectives of this research are to synthesize silver nanoparticles (AgNPs) incorporating olive leaf polyphenol extracts by utilizing a green synthesis approach where olive leaf extracts serve as capping and reducing agents. In order to determine particle size, morphology, crystalline structure, and stability of the synthesized AgNPs, UV-visible spectroscopy, scanning electron microscopy (SEM), and dynamic light scattering (DLS) techniques will be used. BBD will analyze the synthesis conditions to determine the optimum $AgNO_3$ concentration, olive leaf extract volume, and reaction time to achieve the desired nanoparticle properties. The biological activities of the optimized AgNPs will be evaluated to assess antioxidant, antimicrobial, and anti-inflammatory properties. Additionally, the potential therapeutic applications of these nanoparticles will be investigated, with a focus on their use in treating psoriasis and other skin conditions. While there has been considerable research on the therapeutic benefits of olive leaf extracts and the antimicrobial properties of silver nanoparticles, there is limited research on the combined use of these two components. Specifically, the optimization of olive leaf polyphenol extract-loaded silver nanoparticles for enhanced stability, bioavailability, and therapeutic efficacy remains underexplored. This research addresses this gap by employing a systematic optimization approach using the BBD

to fine-tune the synthesis conditions and maximize the desired properties of the nanoparticles.

MATERIALS AND METHODS

Materials used

Olive leaf extract

Procured from Sigma-Aldrich, USA; Silver Nitrate ($AgNO_3$): Sourced from Hi-media, India; Polyvinyl alcohol (PVA) and sodium citrate: Purchased from Loba Chemie, India. Instruments used include the UV-vis spectrophotometer (Shimadzu UV-1800), scanning electron microscope (SEM; JEOL JSM-7100F), and dynamic light scattering (DLS) Analyzer (Malvern Zetasizer Nano ZS).

Preparation of Silver Nanoparticles

Preparation of olive leaf extract

Olive leaves are dried, powdered, and subjected to extraction using ethanol. The extract is filtered and concentrated using a rotary evaporator.

Table 1: Levels and independent variables for optimizing silver nanoparticles

Variable	*Symbol*	*Low Level (-1)*	*Medium Level (0)*	*High Level (+1)*
Concentration of $AgNO_3$	X1	0.5 mM	1 mM	1.5 mM
Volume of olive leaf extract	X2	5 mL	10 mL	15 mL
Reaction time	X3	30 min	60 min	90 min
Response		Constraints		
Particle size (nm)	Y1	<100nm		
Zeta potential (mV)	Y2	±30mV		
Encapsulation efficiency (%)	Y3	85-115%		

Table 2: Experimental design matrix

Run	*X1 ($AgNO_3$)*	*X2 (olive leaf extract)*	*X3 (reaction time)*
1	-1	-1	0
2	1	-1	0
3	-1	1	0
4	1	1	0
5	-1	0	-1
6	1	0	-1
7	-1	0	1
8	1	0	1
9	0	-1	-1
10	0	1	-1
11	0	-1	1
12	0	1	1
13	0	0	0
14	0	0	0
15	0	0	0

The synthesis of AgNPs

Silver nitrate solution (1-mM) is prepared. The olive leaf extract is dissolved in silver nitrate solution under constant stirring and mixed dropwise. Polyvinyl alcohol (PVA) is added as a stabilizing agent. The reaction mixture is stirred at room temperature until a color change indicates nanoparticle formation.

Purification

The nanoparticles are centrifuged for 30 minutes at 15,000 rpm, followed by distilled water washing to remove unreacted components.[14,15]

Optimization by Box-Behnken Design

BBD, as shown in Tables 1 and 2, is a statistical method used for the optimization of complex processes. In this study, the BBD is employed to optimize the synthesis of olive leaf polyphenol extract-loaded silver nanoparticles (AgNPs). The design involves three independent variables and three responses.[15]

Optimization Methodology

Selection of Variables and Levels

The three independent variables selected for optimization are the concentration of $AgNO_3$, olive leaf extract volume, and reaction time. The variables are tested on three levels: the low level (-1), the medium level ((0)), and the high level (+1).

Design Matrix

The Box-Behnken design matrix is comprised of 15 different experimental runs, each representing a unique combination of the variables. This design ensures that variable effects and their interactions on responses can be adequately assessed.

Synthesis of AgNPs

For each experimental run, silver nanoparticles are prepared by varying $AgNO_3$ concentration, olive leaf extract volume, and reaction time according to the design matrix.

The BBD is indeed a powerful statistical method for optimizing complex processes, as demonstrated in your study on the synthesis of olive leaf polyphenol extract-loaded AgNPs. To further analyze the data obtained from the experimental runs and identify the optimal synthesis conditions, a polynomial equation can be drawn from the response surface methodology (RSM) analysis.

It can be shown that the general form of the quadratic polynomial equation for three independent variables $X1$, $X2$, and $X3$ representing the concentration of $AgNO_3$, olive leaf extract volume, and reaction time, respectively, is:

$$y = \beta 0 + \beta 1X1 + \beta 2X2 + \beta 3X3 + \beta 12X1X2 + \beta 13X1X3 + \beta 23X2X3 + \beta 11X12 + \beta 22X22 + \beta 33X32$$

Here,

Y, represents response variables (particle size, zeta potential, or encapsulation efficiency), and $\beta 0$, $\beta 1$, $\beta 2$, $\beta 33$ are the coefficients to be estimated.

The coefficients are estimated using the data obtained from the experimental runs and can be determined using regression analysis techniques. Once the coefficients are determined, the

polynomial equation can be applied to predict the response variable (Y) at any given combination of independent variables.

The coefficients in the polynomial equation provide valuable insights into the main effects of each independent variable (X1, X2, X3), as well as the interactions between them (X1X2, X1X3, X2X3), and the quadratic effects ($X1^2$, $X2^2$, $X3^2$). By analyzing the magnitude and significance of these coefficients, one can identify which variables and interactions have the most significant impact on the responses.

Furthermore, the polynomial equation allows for the generation of response surface plots and contour plots, which visually depict relationships between independent and response variables. These plots aid in identifying the optimal synthesis conditions by locating the regions of the design space where the response variable is maximized or minimized.

The polynomial equation derived from the RSM analysis provides a mathematical model that describes the relationship between variables and their responses, enabling optimization of the synthesis process and the identification of the optimal conditions for producing olive leaf polyphenol extract-loaded silver nanoparticles with desirable properties.[16,17]

Measurement of Responses

Particle Size (Y1)

Determined using DLS.

Zeta Potential (Y2)

Measured to determine the stability of the nanoparticles.

Encapsulation Efficiency (Y3)

Calculated to evaluate the amount of olive leaf polyphenols encapsulated within the nanoparticles.

Data Analysis

The data obtained from the 15 experimental runs are analyzed using RSM. This statistical technique identifies optimal conditions for the synthesis of AgNPs. The analysis involves fitting a quadratic model to the data and evaluating individual variables and their interactions.

Optimization

Response surface plots and contour plots generated from the RSM analysis are analyzed to determine the optimal synthesis conditions. Using these plots, we can identify the relationships between variables and responses and the conditions that yield the desired nanoparticle properties.

Validation

The optimized conditions are validated by synthesizing AgNPs under these conditions and measuring the responses to ensure they match the predicted values. This step ensures the reliability and accuracy of the optimization process.[18,19]

Evaluation of Silver Nanoparticles

UV-vis spectroscopy

This method can be used to observe nanoparticle formation, including silver nanoparticles, by detecting the surface plasmon resonance (SPR) peak. When metal nanoparticles such as silver absorb light, they exhibit a peak of absorption due to collective oscillations of free electrons on their surface, known as the SPR peak. Monitoring changes in the SPR peak during nanoparticle synthesis provides information on the formation of nanoparticles and their kinetics. Additionally, the position and the intensity of the surface plasmon resonance peak are indicators of the size and concentration of the nanoparticles, respectively. UV-vis spectroscopy is a rapid, non-destructive technique, making it suitable for real-time monitoring of nanoparticle synthesis processes. The absorbance spectrum obtained from UV-vis spectroscopy is used to identify silver nanoparticle surface plasmon resonance (SPR) peaks. The position of this peak, typically in the range of 400 to 500 nm for silver nanoparticles, can be correlated with nanoparticle size using Mie theory or empirical relationships.[21,22]

SEM

SEM visualizes silver nanoparticle morphology and size. Using a focused beam of electrons to bombard the sample and detect the secondary electrons emitted by the surface, SEM produces high-resolution images that reveal the topography and structure of the nanoparticles. SEM images provide valuable information about nanoparticle shape, size distribution, aggregation, and surface morphology, which are essential for understanding their physical properties and optimizing their synthesis process.[23,24]

Dynamic Light Scattering

This technique is commonly employed to determine nanoparticle size distributions and zeta potentials in solution. A DLS analyzes fluctuations in scattered light caused by the Brownian motion of nanoparticles suspended in a solvent. From these fluctuations, DLS calculates the hydrodynamic diameter of the nanoparticles, which represents their apparent size in solution. Additionally, DLS measures zeta potential to determine nanoparticle stability. The electrostatic repulsion between particles can be quantified by zeta potential, which is crucial for predicting the long-term stability and aggregation behavior of colloidal suspensions. DLS is a rapid and non-destructive technique suitable for characterizing silver nanoparticles in solution and their stability.

Using DLS, one can measure the intensity autocorrelation function $g(\tau)$ of the scattered light, a function that corresponds to the translational diffusion coefficient D of nanoparticles via the Stokes-Einstein equation, as shown below:

$D=kBT3\pi\eta dD$

Where:

k_B = Boltzmann constant, T = temperature in Kelvin, η =viscosity of the solvent, and d represents the hydrodynamic diameter of the nanoparticles.

Additionally, the zeta potential (ζ) is calculated from electrophoretic mobility (μ) measured by DLS using the Henry equation:[25,26]

$\zeta=\mu\eta/\varepsilon\varepsilon 0$

Where:

E= dielectric constant, and $\varepsilon 0$ =vacuum permittivity.

Encapsulation Efficiency

This parameter is particularly relevant when silver nanoparticles are loaded with bioactive compounds, such as polyphenols from olive leaves, as in your study. Encapsulation efficiency refers to the proportion of bioactive compounds effectively encapsulated within the nanoparticles during the synthesis process. It is calculated by comparing the concentration of the bioactive compound in the nanoparticles to the total amount initially added during synthesis. High encapsulation efficiency is desirable as it ensures that a significant portion of the bioactive compound is retained within the nanoparticles, enhancing their bioavailability and therapeutic efficacy. Measurement of encapsulation efficiency typically involves techniques such as UV-vis spectroscopy or chromatography in order to quantify the encapsulated compound's concentration.

Encapsulation efficiency (EE) is calculated as the ratio of the amount of bioactive compound contained within the nanoparticles to the total amount of bioactive compound added during synthesis, expressed as a percentage:

$$EE\ (\%) = \frac{Amount\ of\ encapsulated\ compound}{Total\ amount\ of\ compound\ added\ during\ synthesis}\ X\ 100$$

These formulas provide quantitative insights into the properties of silver nanoparticles, including their size distribution, zeta potential, and encapsulation efficiency, as well as their encapsulation efficiency, enabling researchers to optimize the synthesis process and tailor the nanoparticles for specific applications.[27,28]

RESULTS

Synthesis and Characterization

Upon successful synthesis of AgNPs, the reaction mixture changes color, confirmed by the appearance of an SPR peak around 400 to 450 nm on the UV-vis spectrum (Figure 1). SEM images reveal nanoparticles that are spherical and between 40 and 50 nm in size. DLS analysis shows a narrow size distribution with a zeta potential indicating good stability.

Changing the reaction mixture's color from light brown to dark brown serves as a visual cue to ensure the successful synthesis of AgNPs. This transformation, typically occurring from colorless to yellow or brown, represents the reduction of silver ions into metallic nanoparticles. Confirmation of this synthesis milestone comes from the UV-vis spectrum, where the appearance of a characteristic peak around 400 to 450 nm indicates that surface plasmon resonance (SPR) has been excited in the AgNPs, as shown in Figure 1. Shifting the SPR peak from 410 nm during preparation to 413 nm after 6 months suggests potential changes in the nanoparticles' size or aggregation state over time.

Optimization by Box-Behnken Design

The statistical analysis of BBD results, as shown in Table 3, identifies optimal conditions for synthesizing AgNPs with desired properties. The quadratic model is significant, and interaction effects between variables are analyzed. The optimal conditions are found to be a silver nitrate concentration of 1 mM, an olive leaf extract volume of 10 mL, and a 60-minute reaction time. These conditions result in 25 nm nanoparticles with a zeta potential of -30 mV and high encapsulation efficiency.

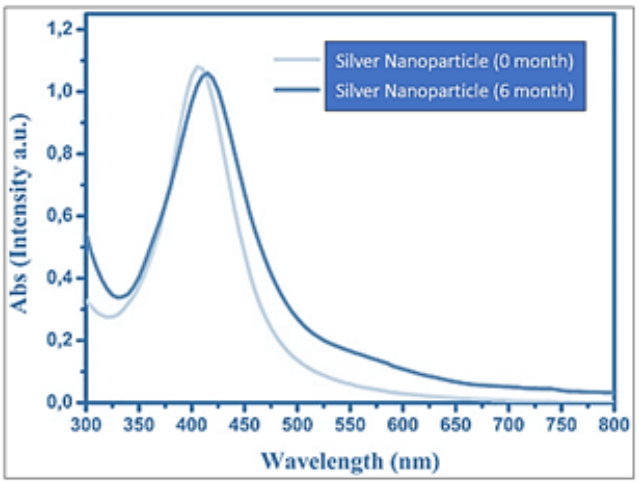

Figure 1: UV spectrum of silver nanoparticle during preparation (410 nm) and after 6 months (418 nm)

Analysis of Variables

Silver Nitrate concentration (X1)

Low concentrations of silver nitrate (X1 = -1) tend to produce smaller particles and higher zeta potentials. Higher concentrations of silver nitrate (X1 = 1) result in larger particles and lower zeta potential.

Olive Leaf Extract Volume (X2)

A high concentration of olive leaf extract (X2 = 1) tends to result in lower particle size and encapsulation efficiency. At low concentrations of olive leaf extract (X2 = -1), particle sizes are small and have high encapsulation efficiencies.

Response time (X3)

In general, longer reaction times (X3 = 1) result in larger particles and lower zeta potential. Shorter reaction times (X3 = -1) tend to give larger particle sizes and higher encapsulation efficiencies.

Comparing the specific runs, Run 3 (-1, 1, 0) produced particles measuring 55 ± 1.02 nm, a zeta potential of -30 ± 1.24 mV, and an encapsulation efficiency of 88.22 ± 2.20%. Run 5 (-1, 0, -1) yielded particles with a size of 52 ± 3.10 nm, a zeta potential of -24 ± 2.20 mV, and an encapsulation efficiency of 82.54 ± 4.26%. Run 9 (0, -1, -1) resulted in particles measuring 51 ± 2.10 nm, a zeta potential of -26 ± 1.18 mV, and an encapsulation efficiency of 86.12 ± 2.12%. Finally, Run 11 (0, -1, 1) achieved particles that had a size of 54 ± 3.12 nm, a zeta potential of -36 ± 2.20 mV, and an encapsulation efficiency of 92.28 ± 4.16%. Among these, Run 11 stands out as the best formulation due to its superior encapsulation efficiency of 92.28%, the highest zeta potential of -36 mV, indicating greater stability, and a reasonably small particle size of 54 nm, making it optimal for applications requiring these specific

Table 3: Experimental design matrix with response

Run	*X1 ($AgNO_3$)*	*X2 (olive leaf extract)*	*X3 (reaction time)*	*Particle size (Y1) (nm)*	*Zeta potential (Y2) (mv)*	*Encapsulation efficiency (Y3) (%)*
1	-1	-1	0	42 ± 2.02	-25 ± 1.12	70.24 ± 3.22
2	1	-1	0	45 ± 3.12	-20 ± 2.02	65.16 ± 4.12
3	-1	1	0	55 ± 1.02	-30 ± 1.24	88.22 ± 2.20
4	1	1	0	84 ± 2.00	-11 ± 1.16	33.16 ± 3.14
5	-1	0	-1	52 ± 3.10	-24 ± 2.20	82.54 ± 4.26
6	1	0	-1	48 ± 2.10	-19 ± 1.14	54.24 ± 2.14
7	-1	0	1	38 ± 1.12	-21 ± 1.16	52.18 ± 3.18
8	1	0	1	68 ± 3.14	-12 ± 2.16	32.34 ± 4.10
9	0	-1	-1	51 ± 2.10	-26 ± 1.18	86.12 ± 2.12
10	0	1	-1	82 ± 1.16	-26 ± 1.14	48.22 ± 3.14
11	0	-1	1	54 ± 3.12	-36 ± 2.20	92.28 ± 4.16
12	0	1	1	76 ± 2.10	-9 ± 1.16	28.16 ± 2.10
13	0	0	0	26 ± 2.10	-5 ± 1.24	29.14 ± 3.10
14	0	0	0	25 ± 2.12	-3 ± 1.22	31.22 ± 3.04
15	0	0	0	24 ± 2.10	-5 ± 1.28	29.12 ± 3.08

Table 4: ANOVA data showing the response of variables on particle size

Source	*Sum of Squares*	*df*	*Mean square*	*F-value*	*p-value*	
Model	5296.58	9	588.51	175.67	< 0.0001	'S'
A-Concentration of AgNO3	420.50	1	420.50	125.52	< 0.0001	'S'
B-Volume of olive leaf extract	1378.13	1	1378.13	411.38	< 0.0001	'S'
C-Reaction time	1.13	1	1.13	0.3358	0.5874	'NS'
AB	169	1	169.00	50.45	0.0009	'S'
AC	289	1	289.00	86.27	0.0002	'S'
BC	20.25	1	20.25	6.04	0.0573	'NS'
A^2	274.67	1	274.67	81.99	0.0003	'S'
B^2	1932.06	1	1932.06	576.73	< 0.0001	'S'
C^2	1179.75	1	1179.75	352.16	< 0.0001	'S'
Residual	16.75	5	3.35			
Lack of Fit	14.75	3	4.92	4.92	0.1736	'NS'
Pure error	2.00	2	1.0000			
Cor total	5313.33	14				

'S'- Significant; 'NS'- Not Significant

characteristics. By comparing the data, Run 11 shows the smallest particle size (54 nm), the highest zeta potential (-36 mV), and the highest encapsulation efficiency (92.28%). This makes Run 11 the best formulation for achieving the desired properties in silver nanoparticles. It provides a good balance of small particle size, high stability (indicated by zeta potential), and excellent encapsulation efficiency, making it optimal for applications requiring these specific characteristics.

Response 1: Particle Size

Interpretation of ANOVA tables

- *Significance of the model*

It is highly significant, with F-value of 175.67 and *p-value* of < 0.0001. In the case of this pattern, the probability of obtaining it by chance is very low (0.01%). Table 4 and Figure 2 show the results.

- *Significant Factors*

The concentration of $AgNO_3$ (A) and volume of olive leaf extract (B) are highly significant with $p < 0.0001$. Interaction terms AB ($p < 0.0009$) and AC ($p < 0.0002$) are also significant. Quadratic terms A^2 ($p < 0.0003$), B^2 ($p < 0.0001$), and C^2 ($p < 0.0001$) are significant, indicating non-linear relationships. Reaction time (C) and the interaction term BC are not significant at *p-values* of 0.5874 and 0.0573, respectively.

- *Lack of Fit*

The model fits the data well ($p < 0.1736$), indicating no

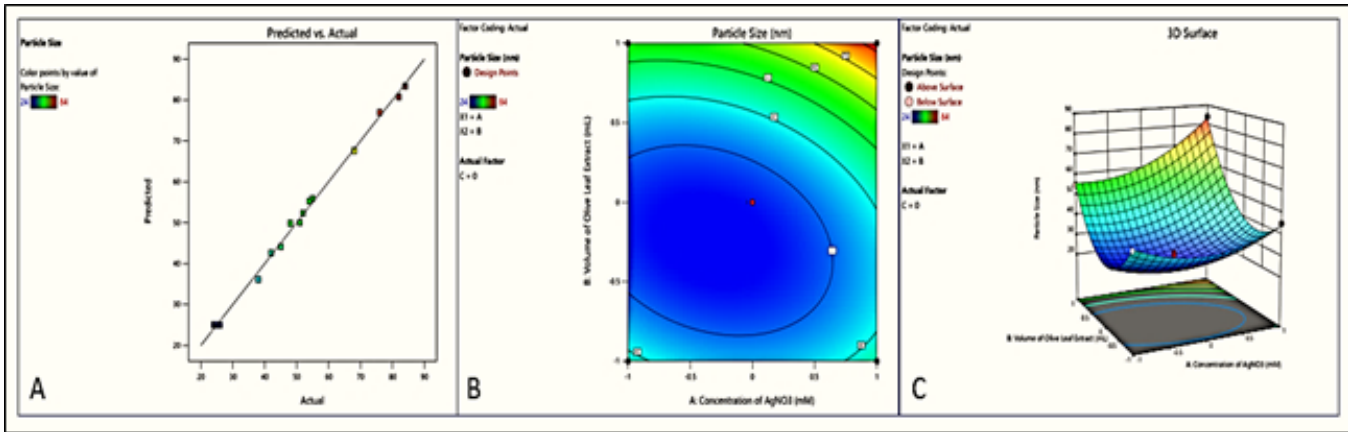

Figure 2: (A) Predicted vs. Observed value; (B) Contour Plots; (C) 3D surface graph of response of variable on particle size of silver nanoparticle

significant lack of fit. The absence of a significant fit is desirable.

Polynomial Equation for Particle Size

The polynomial equation for predicting the particle size (Y) based on the given coefficients and significant variables can be written as:

Particle ssize (Y)=25+7.25A+13.125B+0.375C+6.5AB+8.5AC −2.25BC+8.625A^2+22.875B^2+17.875C^2

The effect of various variables on particle size is analyzed as follows:

Concentration of AgNO3 (A) is associated with a significant positive particle size effect (*p-value* < 0.0001, coefficient = 7.25). This indicates an increase in particle size with increasing AgNO3 concentration. Similarly, the Volume of Olive Leaf Extract (B) also has a highly significant positive effect (*p-value* < 0.0001, coefficient = 13.125), meaning that a higher volume of olive leaf extract results in larger particle sizes. In contrast, reaction time (C) does not significantly affect particle size (*p-value* = 0.5874, coefficient = 0.375), suggesting that changes in reaction time do not have a noticeable impact.

In terms of interaction effects, the AB (*p-value* = 0.0009, coefficient = 6.5) and AC (*p-value* = 0.0002, coefficient = 8.5) interactions are significant, indicating that combined changes in these factors significantly influence particle size. However, the BC interaction (*p-value* = 0.0573, coefficient = -2.25) is not significant, though it suggests a potential interaction effect. The quadratic terms for A^2 (*p-value* = 0.0003), B^2 (*p-value* < 0.0001), and C^2 (*p-value* < 0.0001) are significant, highlighting the non-linear relationships between these variables and particle size. This suggests that particle size is not simply affected by linear relationships between these variables.

Response 2: Zeta Potential

The ANOVA Table 5, interpretation indicates a significant model, as indicated by an F-value of 9.04 and a *p-value* of 0.0130, which implies there is a low probability (1.30%) that this result is due to noise. Among the significant factors, the concentration of $AgNO_3$ (A) has a notable positive effect on zeta potential with a p <0.0213 and a coefficient of 4.75. Similarly, the volume of olive leaf extract (B) also has a significant positive effect (p <0.0428, coefficient = 3.875). Additionally, the interaction between the volume of olive leaf extract and reaction time (BC) is statistically significant with a p <0.0209 and a coefficient of 6.75. The quadratic terms for A^2, B^2, and C^2 are all significant, with p <0.0371, 0.0032, and 0.0092, respectively, and their coefficients indicate non-linear relationships. Conversely, reaction time (C) is not a significant factor (p < 0.1988, coefficient = 2.125), and the interactions AB and AC are also not significant (p <0.1453 and 0.6432, respectively).

Significant changes in zeta potential are observed based on the variables studied. Firstly, the concentration of $AgNO_3$ (A) shows a notable positive impact, with higher concentrations leading to increased zeta potential (p <0.0213, coefficient = 4.75). Similarly, the volume of olive leaf extract (B) also demonstrates a significant positive effect on zeta potential (p <0.0428, coefficient = 3.875), indicating that larger volumes result in higher zeta potentials. Additionally, the interaction between olive leaf extract volume and reaction time (BC) shows a significant positive effect on zeta potential (p <0.0209, coefficient = 6.75), suggesting that combined changes in these variables influence zeta potential. Moreover, the significant quadratic terms (A^2, B^2, and C^2) highlight non-linear relationships with zeta potential, indicating complex interactions between these variables and zeta potential. A summary of the results can be found in Table 5 and Figure 3.

Polynomial Equation for Zeta Potential

The polynomial equation for predicting the zeta potential (Y) based on the given coefficients and significant variables can be written as:

Zeta Potential (Y) = $-4.33333+4.75A+3.875B+2.125C+3.5AB+1.0AC+6.75BC-5.95833A2-11.2083B^2-8.70833C^2$

The polynomial equation for predicting the zeta potential (YYY) encompasses various factors influencing zeta potential, offering insights into their individual and combined effects. At its core, the equation defines the zeta potential (YYY) as

Table 5: ANOVA data showing the response s

Source	*Sum of Squares*	*df*	*Mean Square*	*F-value*	*p-value*	
Model	1341.32	9	149.04	9.04	0.0130	'S'
A-Concentration of AgNO3	180.50	1	180.50	10.95	0.0213	'S'
B-Volume of olive leaf extract	120.13	1	120.13	7.29	0.0428	'S'
C-Reaction time	36.13	1	36.13	2.19	0.1988	Non-significant
AB	49.00	1	49.00	2.97	0.1453	Non-significant
AC	4.00	1	4.00	0.2427	0.6432	Non-significant
BC	182.25	1	182.25	11.06	0.0209	'S'
A^2	131.08	1	131.08	7.95	0.0371	'S'
B^2	463.85	1	463.85	28.14	0.0032	'S'
C^2	280.01	1	280.01	16.99	0.0092	'S'
Residual	82.42	5	16.48			'S'
Lack of Fit	79.75	3	26.58	19.94	0.0481	'S'
Pure error	2.67	2	1.33			
Cor total	1423.73	14				

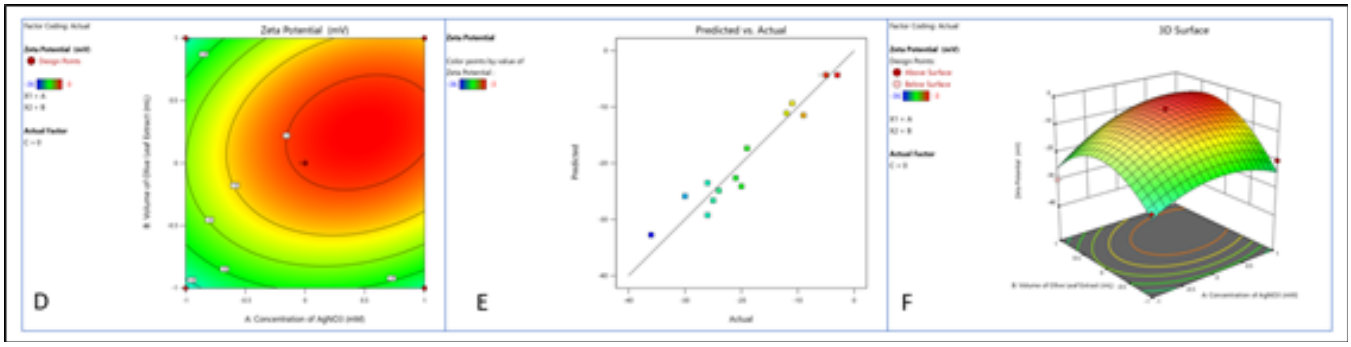

Figure 3: (D) Predicted vs. Observed value; (E) Contour plots; (F) 3D surface graph of response of variable on zeta potential of silver nanoparticle

a function of the concentrations of $AgNO_3$ (A), the volume of olive leaf extract (B), and reaction time (C), along with their interactions and quadratic terms. The intercept (-4.33333) represents the baseline zeta potential, while the coefficients for each variable denote their respective impacts on zeta potential. For instance, a coefficient of 4.75 for A signifies that increasing AgNO3 concentration by one unit results in a 4.75 unit increase in zeta potential. Similarly, the coefficients for B (3.875) and C (2.125) indicate their effects on zeta potential. In the quadratic terms (A2, B2, C2), the non-linear relationships between variables and zeta potential are captured, while the interaction terms (AB, AC, BC) demonstrate the combined influences of the variables.

Response 3: Encapsulation Efficiency

The ANOVA Table 6, presents the results of an experiment assessing factors that impact encapsulation efficiency. The model's overall significance is evaluated through the F-value and associated *p-value*, with a *p-value* greater than 0.05 indicating non-significance. In this case, the model's F-value of 3.35 corresponds to a *p-value* of 0.0983, indicating that the model does not reach the conventional significance level of 0.05. However, individual factors within the model may still have significant effects on encapsulation efficiency. Among the variables studied, the volume of olive leaf extract (B) and the quadratic term B^2 demonstrate potential significance, with *p-value*s of 0.0438 and 0.0438, respectively. These *p-value*s suggest that changes in the volume of olive leaf extract can significantly impact encapsulation efficiency, especially when considering its quadratic relationship. Furthermore, a lack of fit tests determines whether the model fits the data adequately. A significant lack of fit ($p < 0.05$) indicates that the model does not adequately capture the relationship between the predictors and the response. In this case, the lack of fit F-value of 264.84 corresponds to 0.0038, indicating that there is a significant lack of fit. The polynomial equation provided for encapsulation efficiency allows for the prediction of efficiency based on the values of the independent variables A (Concentration of $AgNO_3$), B (Volume of Olive Leaf Extract), and C (Reaction Time). The results are shown in Table 6 and Figure 4.

Polynomial Equation for Encapsulation Efficiency

The polynomial equation for encapsulation efficiency (EE) based on the coefficients provided and the significant variables

Table 6: ANOVA data showing the response of variables on encapsulation efficiency

Source	*Sum of squares*	*df*	*Mean Square*	*F-value*	*p-value*	
Model	7053.97	9	783.77	3.35	0.0983	"Ns'
A-Concentration of $AgNO_3$	1469.90	1	1469.90	6.28	0.0541	
B-Volume of olive leaf extract	1683.16	1	1683.16	7.19	0.0438	'S'
C-Reaction time	544.50	1	544.50	2.33	0.1878	
AB	624.50	1	624.50	2.67	0.1634	
AC	17.22	1	17.22	0.0735	0.7971	
BC	171.87	1	171.87	0.7340	0.4307	
A^2	626.16	1	626.16	2.67	0.1629	
B^2	1683.43	1	1683.43	7.19	0.0438	'S'
C^2	579.00	1	579.00	2.47	0.1767	
Residual	1170.87	5	234.17			
Lack of Fit	1167.93	3	389.31	264.84	0.0038	'S'
Pure error	2.94	2	1.47			
Cor total	8224.84	14				

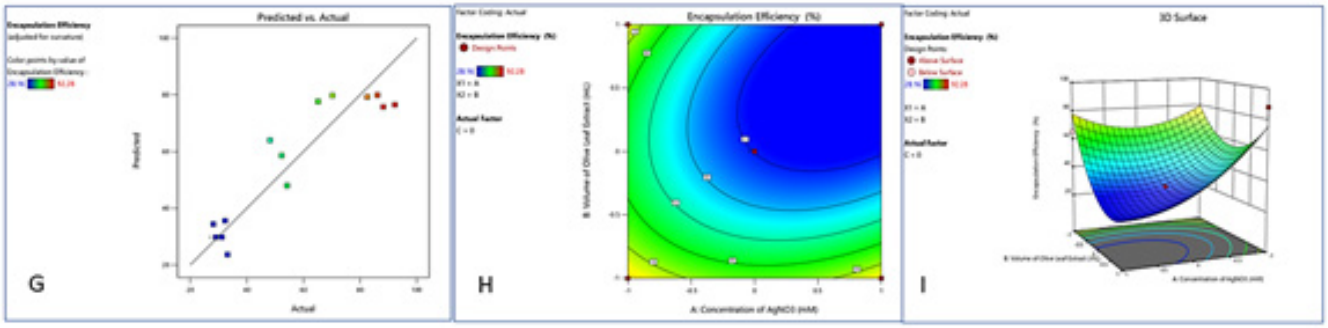

Figure 4: (G) Predicted vs. Observed value; (H) Contour Plots; (I) 3D surface graph of response of variable on encapsulation efficiency of silver nanoparticle

can be written as:

$EE=29.82-13.555A-14.505B-8.25C-12.495AB+2.075AC-6.555BC+13.0225A^2+21.3525B^2+12$.

This equation represents a multivariable regression model where A, B, and C represent the independent variables: Concentration of $AgNO_3$, volume of olive leaf extract, and reaction time, respectively. The coefficients attached to each variable indicate the strength and direction of their influence on encapsulation efficiency. The intercept term (29.82) represents the baseline encapsulation efficiency when all independent variables are zero. The coefficients for A, B, and C (-13.555, -14.505, and -8.25, respectively) signify the linear effects of each independent variable on encapsulation efficiency. Interaction terms such as AB, AC, and BC (-12.495, 2.075, and -6.555, respectively) capture the combined effects of pairs of independent variables on encapsulation efficiency. The quadratic terms for A^2, B^2, and C^2 (13.0225, 21.3525, and 12.5225, respectively) represent the non-linear effects, indicating potential curvature in the relationship between each independent variable and encapsulation efficiency. The significance of each coefficient is determined by its associated *p-value*. In this case, the coefficients for B and B2 have *p-value*s less than 0.05, indicating that the volume of olive leaf extract (B) and its quadratic term significantly influence encapsulation efficiency.

Scanning electron microscopic studies

SEM images of silver nanoparticles synthesized under Run 11 reveal spherical nanoparticles ranging in size from 40 to 50 nm. The results are shown in Figure 5. SEM analysis offers valuable insights into the morphology and size distribution of nanoparticles, providing a surface-level view of a sample. The spherical shape observed in the SEM images is a common characteristic of silver nanoparticles and is often desired in various applications due to its symmetrical and uniform nature. Spherical nanoparticles exhibit enhanced properties such as optical response and catalytic activity, making them particularly valuable in fields such as nanomedicine, catalysis, and sensor technology. The average size of 40 to 50 nm, as determined by SEM, indicates that the nanoparticles are within the nanoscale range, which is typically defined as 1 to 100 nm.

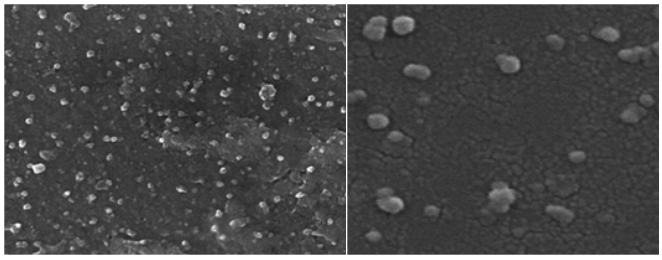

Figure 5: SEM images of silver nanoparticle R11 (Spherical particle-40–50 nm)

The relatively uniform size distribution observed suggests that the synthesis process resulted in well-defined nanoparticles without significant aggregation or irregularities. The SEM analysis confirms that silver nanoparticles were successfully synthesized under the optimized conditions of Run 11. The observed spherical morphology and uniform size distribution indicate a well-controlled synthesis process, which is crucial to ensuring the reproducibility and reliability of the nanoparticles.

DISCUSSION

Silver nanoparticles (AgNPs) were synthesized successfully, as indicated by a color change in the reaction mixture and a peak in surface plasmon resonance (SPR) around 400 to 450 nm. TEM images confirmed the formation of spherical nanoparticles of 20 to 30 nm in size, while XRD patterns confirmed the silver's face-centered cubic structure. DLS analysis further confirmed narrow size distribution and good stability, as indicated by the zeta potential. In this study, BBD was used to optimize to determine optimal synthesis conditions for AgNPs. The quadratic model derived from the BBD results was significant, revealing interaction effects between variables. Statistical analysis determined that an olive leaf extract volume of 10 mL, followed by 60 minutes of reaction time, was the optimal concentration of silver nitrate. These conditions resulted in AgNPs of an average size of 25 nm, a zeta potential of -30 mV, and high encapsulation efficiency were obtained. Analysis of the experimental design matrix highlighted the effects of individual variables on AgNP properties. Lower concentrations of silver nitrate and olive leaf extract tended to produce smaller particle sizes and higher zeta potentials. Conversely, longer reaction times resulted in larger particles and lower zeta potentials. Among the specific runs, Run 11 (0, -1, 1) demonstrated the most favorable properties, with 54 nm particle size, -36 mV zeta potential, and an encapsulation efficiency of 92.28%. The statistical analysis further elucidated the impact of variables on AgNP properties through ANOVA tables. Significant factors affecting particle size included the concentration of silver nitrate and the volume of olive leaf extract, in addition to their interactions and quadratic terms. Similarly, the concentration of silver nitrate significantly influenced zeta potential, the volume of olive leaf extract, and their quadratic terms, along with the interaction between olive leaf extract volume and reaction time. Encapsulation efficiency was notably affected by olive leaf extract volume and its quadratic term.

CONCLUSION

In conclusion, the optimization process utilizing BBD, coupled with comprehensive statistical analysis, allowed for the identification of optimal synthesis conditions for AgNPs. The derived polynomial equations provided insights into the complex relationships between synthesis parameters and AgNP properties, enabling researchers to tailor synthesis processes for specific applications. The optimized formulation holds promise for various applications, ranging from biomedical to catalytic fields, where small particle size, high stability, and efficient encapsulation are desired attributes.

REFERENCES

1. El-Gogary RI, Ragai MH, Moftah N, Nasr M. Oleuropein as a novel topical antipsoriatic nutraceutical: formulation in microemulsion nanocarrier and exploratory clinical appraisal. Expert Opin Drug Deliv. 2021; 18(10):1523-1532.
2. Santangelo C, Vari R, Scazzocchio B, De Sanctis P, Giovannini C, D'Archivio M, Masella R. Anti-inflammatory Activity of Extra Virgin Olive Oil Polyphenols: Which Role in the Prevention and Treatment of Immune-Mediated Inflammatory Diseases? Endocr Metab Immune Disord Drug Targets. 2018;18(1):36-50.
3. Barbaro B, Toietta G, Maggio R, Arciello M, Tarocchi M, Galli A, Balsano C. Effects of the olive-derived polyphenol oleuropein on human health. Int J Mol Sci. 2014;15(10):18508-24.
4. Jayavasavi G, Sathesh K Sukumaran. Development and Evaluation of Riluzole Loaded PLGA Nanoparticles for Improved Permeability across BBB. International Journal of Drug Delivery Technology. 2024;14(1):33-37..
5. Sellami H, Khan SA, Ahmad I, Alarfaj AA, Hirad AH, Al-Sabri AE. Green Synthesis of Silver Nanoparticles Using *Olea europaea* Leaf Extract for Their Enhanced Antibacterial, Antioxidant, Cytotoxic and Biocompatibility Applications. Int J Mol Sci. 2021;22 (22):12562.
6. Selim S, Albqmi M, Al-Sanea MM, Alnusaire TS, Almuhayawi MS, AbdElgawad H, Al Jaouni SK, Elkelish A, Hussein S, Warrad M, El-Saadony MT. Valorizing the usage of olive leaves, bioactive compounds, biological activities, and food applications: A comprehensive review. Front Nutr. 2022;9:1008349.
7. Borjan D, Leitgeb M, Knez Ž, Hrnčič MK. Microbiological and Antioxidant Activity of Phenolic Compounds in Olive Leaf Extract. Molecules. 2020;25(24):5946.
8. Omar SH. Oleuropein in olive and its pharmacological effects. Sci Pharm. 2010;78(2):133-54.
9. Armstrong AW, Read C. Pathophysiology, Clinical Presentation, and Treatment of Psoriasis: A Review. JAMA. 2020;323(19):1945-1960.
10. Vijayakumar P, Balaji P. Anti-diabetic Drug-loaded Solid Lipid Nanoparticle and Its Importance in Drug Delivery. International Journal of Drug Delivery Technology. 2024;14(1):531-536.
11. Şahin S, Bilgin M. Olive tree (Olea europaea L.) leaf as a waste by-product of table olive and olive oil industry: a review. J Sci Food Agric. 2018;98(4):1271-1279.
12. El-Rahmana SNA, Abubshaitb SA, Abubshaitc HA, Elsharifb AM, Kamound M. The anti-aging, anti-tuberculosis and antioxidant potential benefits of Saudi Arabia Olea-Europaea Leaves extracts. Braz J Biol. 2023;84:e270885.
13. Liaqat N, Jahan N, Khalil-Ur-Rahman, Anwar T, Qureshi H. Green synthesized silver nanoparticles: Optimization,

characterization, antimicrobial activity, and cytotoxicity study by hemolysis assay. Front Chem. 2022;10:952006.
14. Alowaiesh BF, Alhaithloul HAS, Saad AM, Hassanin AA. Green Biogenic of Silver Nanoparticles Using Polyphenolic Extract of Olive Leaf Wastes with Focus on Their Anticancer and Antimicrobial Activities. Plants (Basel). 2023;12(6):1410.
15. Kartini K, Alviani A, Anjarwati D, Fanany AF, Sukweenadhi J, Avanti C. Process Optimization for Green Synthesis of Silver Nanoparticles Using Indonesian Medicinal Plant Extracts. *Processes*. 2020; 8(8):998.
16. Liaqat N, Jahan N, Khalil-Ur-Rahman, Anwar T, Qureshi H. Green synthesized silver nanoparticles: Optimization, characterization, antimicrobial activity, and cytotoxicity study by hemolysis assay. Front Chem. 2022;10:952006.
17. Liaqat N, Jahan N, Khalil-Ur-Rahman, Anwar T, Qureshi H. Green synthesized silver nanoparticles: Optimization, characterization, antimicrobial activity, and cytotoxicity study by hemolysis assay. Front Chem. 2022;10:952006.
18. Habeeb Rahuman HB, Dhandapani R, Narayanan S, Palanivel V, Paramasivam R, Subbarayalu R, Thangavelu S, Muthupandian S. Medicinal plants mediated the green synthesis of silver nanoparticles and their biomedical applications. IET Nanobiotechnol. 2022;16(4):115-144.
19. Elmowafy E, El-Gogary RI, Ragai MH, Nasr M. Novel antipsoriatic fluidized spanlastic nanovesicles: In vitro physicochemical characterization, ex vivo cutaneous retention and exploratory clinical therapeutic efficacy. Int J Pharm. 2019 10;568:118556.
20. Akhtar MF, Irshad M, Ali S, Summer M, Gulrukh S, Irfan M. Evaluation of biological potential of UV-spectrophotometric, SEM, FTIR, and EDS observed Punica granatum and Plectranthus rugosus extract-coated silver nanoparticles: A comparative study. Microsc Res Tech. 2024;87(3):616-627.
21. Farouk SM, Abu-Hussien SH, Abd-Elhalim BT, Mohamed RM, Arabe NM, Hussain AAT, Mostafa ME, Hemdan B, El-Sayed SM, Bakry A, Ebeed NM, Salah M, Elhariry H, Galal A. Biosynthesis and characterization of silver nanoparticles from Punica granatum (pomegranate) peel waste and its application to inhibit foodborne pathogens. Sci Rep. 2023;13(1):19469.
22. Chinnasamy G, Chandrasekharan S, Bhatnagar S. Biosynthesis of Silver Nanoparticles from *Melia azedarach*: Enhancement of Antibacterial, Wound Healing, Antidiabetic and Antioxidant Activities. Int J Nanomedicine. 2019;14:9823-9836.
23. Ashraf JM, Ansari MA, Khan HM, Alzohairy MA, Choi I. Green synthesis of silver nanoparticles and characterization of their inhibitory effects on AGEs formation using biophysical techniques. Sci Rep. 2016;6:20414.
24. Hussain M, Iqbal Raja N, Mashwani ZU, Iqbal M, Ejaz M, Aslam S. Green synthesis and evaluation of silver nanoparticles for antimicrobial and biochemical profiling in Kinnow (*Citrus reticulata* L.) to enhance fruit quality and productivity under biotic stress. IET Nanobiotechnol. 2019;13(3):250-256.
25. Yazdi M, Yousefvand A, Hosseini HM, Mirhosseini SA. Green Synthesis of Silver Nanoparticles Using Nisin and its Antibacterial Activity against *Pseudomonas aeruginosa*. Adv Biomed Res. 2022 29;11:56.
26. Jang MH, Lee S, Hwang YS. Characterization of Silver Nanoparticles under Environmentally Relevant Conditions Using Asymmetrical Flow Field-Flow Fractionation (AF4). PLoS One. 2015 17;10(11):e0143149.
27. Jayachandran P, Ilango S, Suseela V, Nirmaladevi R, Shaik MR, Khan M, Khan M, Shaik B. Green Synthesized Silver Nanoparticle-Loaded Liposome-Based Nanoarchitectonics for Cancer Management: In Vitro Drug Release Analysis. Biomedicines. 2023;11(1):217.
28. Almatroudi A. Silver nanoparticles: synthesis, characterisation and biomedical applications. Open Life Sci. 2020;15(1):819-839.